Optimized virtual orbital space for highlevel correlated calculations

Ludwik Adamowicz and Rodney J. Bartlett

Citation: The Journal of Chemical Physics **86**, 6314 (1987); doi: 10.1063/1.452468
View online: http://dx.doi.org/10.1063/1.452468
View Table of Contents: http://scitation.aip.org/content/aip/journal/jcp/86/11?ver=pdfcov
Published by the AIP Publishing

Articles you may be interested in

Perturbational treatment of spin-orbit coupling for generally applicable high-level multi-reference methods
J. Chem. Phys. **141**, 074105 (2014); 10.1063/1.4892060

The CMS HighLevel Trigger
AIP Conf. Proc. **1182**, 188 (2009); 10.1063/1.3293780

Highlevel radioactive waste
Phys. Teach. **33**, 450 (1995); 10.1119/1.2344264

Alternative way to dispose of highlevel waste in outer space
AIP Conf. Proc. **324**, 347 (1995); 10.1063/1.47188

Optimized virtual orbital space for highlevel correlated calculations. II. Electric properties
J. Chem. Phys. **88**, 5749 (1988); 10.1063/1.454721

This article is copyrighted as indicated in the article. Reuse of AIP content is subject to the terms at: http://scitation.aip.org/termsconditions. Downloaded to IP: 129.49.170.188 On: Sat, 20 Dec 2014 03:22:48

Optimized virtual ortibal space for high-level correlated calculations[a)]

Ludwik Adamowicz and Rodney J. Bartlett[b)]
Quantum Theory Project, Departments of Chemistry and Physics, University of Florida, Gainesville, Florida 32611

(Received 6 January 1987; accepted 26 February 1987)

The second order Hylleraas functional and a Newton–Raphson orbital optimization technique have been used to generate an active, optimized virtual orbital space (OVOS) of substantially reduced dimension for correlated calculations. Numerical examples for $CH_2(^1A_1)$, C_6H_6, and potential curves for B_2H_6 and H_2O_2 using MBPT and coupled-cluster theory demonstrate that most of the correlation energy can be obtained with a much smaller number of optimized virtual orbitals, and effectively $\sim 100\%$ of the correlation energy if the OVOS result is combined with the exact second-order energy that is evaluated as a byproduct of the OVOS generation. This suggests a potentially wide applicability of the OVOS method in high accuracy quantum mechanical calculations.

I. INTRODUCTION

The vast majority of quantum chemical calculations, which include electron correlation, are performed with the wave function being represented as a linear combination of Slater determinants. Both configuration coefficients, molecular orbital (MO) coefficients, and the primitive (usually atomic orbital, AO) basis which defines the Hilbert space for the problem, can be treated as variables of such expansions. This leads to two of the three fundamental limitations in *ab initio* quantum chemistry—the extent of the configuration expansion and the limitations in the primitive (or MO) basis set. (The third limitation, the number of atoms P leading to $3P$-6 degrees of freedom in a molecule's potential surface is best approached through analytical gradient methods, but is not considered in this paper.)

For a given basis set, the configuration or the "correlation" problem, if viewed as the correction to a Hartree–Fock SCF reference function, can be formally solved by the full CI solution, i.e., all possible up to N-fold excitations for N electrons.[1] Although impractical for any but small "benchmark" examples,[2–4] other methods such as fourth-order many-body perturbation theory (MBPT),[5–8] coupled-cluster theory[9–11] at various levels such as single and double excitation cluster operators (CCSD),[12] and now extended to include triple excitation clusters [CCSDT-1,[13] CCSD + T(CCSD),[14] CCSDT[15]], as well as multireference configuration interaction (MR-CI)[16] have been shown to quite accurately reproduce the full CI in many examples[3,7,11]; but unlike full CI, these methods are applicable for many realistic, chemically interesting problems. Consequently, in this paper we focus on the other fundmental limitation in *ab initio* quantum chemistry, the primitive, and MO basis sets.

The AO basis and the MO basis are actually two different but interconnected problems. Since the full CI results are invariant to any transformation of the AO's, from simple linear algebra, the ultimate result for the energy or another property is solely determined by the choice of primitive basis set. Less complete correlated methods do not have this property, but usually possess a more restrictive set of invariant transformation properties. Separating the molecular orbitals into a set of n_{occ} orbitals said to be occupied, and N_{VIRT} said to be unoccupied in a single determinant reference, CCSD, CCSDT-1, CCSDT, etc., are all invariant to transformations that mix occupied with occupied or virtual with virtual orbitals. (For reasons that will become clear later, we choose to use the term "virtual" for the "excited" orbitals, although this sometimes implies a canonical SCF set of excited orbitals.) Similarly, any truncated CI method that includes *all* excitations at a particular level, like CISD, CISDT, etc., are invariant to such transformations. Each order in MBPT is also, provided that the choice of splitting of the Hamiltonian into $H_0 + V$ is not changed, however, that often means a less natural division of H once the orbitals are rotated, so this type of invariance has not been routinely employed.[17] However, even with an alternative splitting of H by the time MBPT is taken to third and fourth order, for all practical purposes, the invariance to transformations among just the occupied or just the virtual orbitals, manifests itself numerically.[17,18] However, none of the less than full CI methods is invariant to transformations that mix occupied and unoccupied orbitals. So in principle, it is possible to improve the agreement between a correlated method and full CI by simultaneously optimizing the MO's for the problem, as in MCSCF,[19] or perhaps natural-orbital iterations in CI,[20] or as in the orbital optimized CC methods that have been suggested and applied.[12] Once a method includes enough configurations to provide results that approach near agreement with full CI, though, there has to be little to gain from that category of transformations as well. Since, in this paper we are primarily focusing on the CCSD + T(CCSD), CCSDT-1, and MBPT(4) methods that generally show such agreement with full CI,[11] we will not generally address transformations that mix the occupied and virtual space.

Even restricting ourselves to transformations just among the virtual orbitals, the one place where important gains can be achieved is if we can reduce the dimension of

[a)] This research has been supported by the U.S. Office of Naval Research.
[b)] Guggenheim Fellow.

 0021-9606/87/116314-11$02.10 © 1987 American Institute of Physics

This article is copyrighted as indicated in the article. Reuse of AIP content is subject to the terms at: http://scitation.aip.org/termsconditions. Downloaded to IP: 129.49.170.188 On: Sat, 20 Dec 2014 03:22:48

$N_{\rm VIRT}$, but with only an acceptable loss in the accuracy of the final results. To illustrate, MBPT(4) has an asymptotic dependence on the number of orbitals, of $\sim n_{\rm occ}^3 N_{\rm VIRT}^4$, while CCSDT-1's dependence is $\sim n_{\rm occ}^3 N_{\rm VIRT}^4 \times N_{\rm ITS}$ where $N_{\rm ITS}$ is the number of iterations required to reach convergence. CCSDT requires $\sim n_{\rm occ}^3 N_{\rm VIRT}^5 \times N_{\rm ITS}$. Similarly, CCSD and CISD have a $\sim n_{\rm occ}^2 N_{\rm VIRT}^4 \times N_{\rm ITS}$ dependence. If we are able to reduce $N_{\rm VIRT}$ by some factor $x > 1$, $N'_{\rm VIRT} = N_{\rm VIRT}/x$, then we can potentially save $\sim x^4$ in the computer time per iteration, and more for CCSDT or even higher-order approximations. It is also true that the total number of primitive functions $M = n_{\rm occ} + N_{\rm VIRT}$, so if we can reduce to an effective $N'_{\rm VIRT}$ dimension that is manageable without significant loss in accuracy, we can greatly increase M beyond the current level allowed for correlated calculations. This follows because the asymptotic dependence is only $\sim M^4$ for an SCF computation and even less for very large molecules where many of the integrals will be below a small threshold. In practice, then, we are able to use much larger basis sets at the SCF level than for correlated calculations.[21] This fact raises the possibility of trying to attempt to approach complete basis set results for some small examples. Once combined with full CI, such a result would give the "complete" CI result which would be the solution to the nonrelativistic Schrödinger equation.

There have been several previous proposals of ways to obtain improved virtual orbitals for correlated calculations. For example, since the Hartree–Fock SCF occupied orbitals are determind in an effective potential, $V^{\rm eff}$, due to $N-1$ electrons, while the usual virtual orbitals come from an effective potential generated by all N electrons, Kelly[22] proposed a modification using a V^{N-1} potential for the virtual orbitals obtained by excluding one of the occupied orbitals in

$$V^{N-1} = \sum_{j(\neq i)} \int \phi_j^*(2) r_{12}^{-1} (1 - P_{12}) \phi_j(2) d\tau_2.$$

This was generalized by Silver and Bartlett[18] for MBPT, using the form of Hamiltonian of Silverstone and Yin[23] and Huzinaga and Arnau,[24] which define the sum of one particle Hamiltonians to be $H_0 = h + V^{\rm eff} + Q(V - V^{\rm eff})Q$. This permits any choice for V while Q is the projector for the virtual space causing only the virtual orbitals to see the new potential V. Various choices for V including excluding p electrons in an average manner [$\overline{V}^{N-p} = (N-p)N^{-1}V^N$] have been studied numerically by Silver and Bartlett[18] in MBPT.

Another choice would be pseudonatural orbitals,[25] obtained by diagonalizing an approximate density matrix, perhaps constructed form the first-order MBPT wave function. These orbitals, unlike the $\overline{V}^{N-p}$ choice, mix the occupied and excited orbital spaces. However, if one diagonalizes the occupied–occupied and virtual–virtual blocks separately the SCF wave function remains intact. This procedure leads to so-called frozen natural orbitals (FNO).[26] The success of natural orbitals would rest upon the theorem that the natural-orbital CI expansion would give the best approximation to the exact density.[20] Other choices, termed internally consistent (IC) SCF orbitals have been proposed by Davidson,[27] and another improved virtual orbitals (IVO) have been proposed by Hunt and Goddard.[28] The latter two schemes are close conceptually and numerically to the $\overline{V}^{N-p}$ virtual orbitals discussed above.

There is another group of methods,[29] which derive their origin from the K-orbital method developed by Feller and Davidson.[30] The virtual orbital transformation is evaluated by solving Fock-like equations involving the HF exchange potential. The procedure is based upon requiring that the doubly excited determinants have maximum interaction with the reference function.

Each of these different choices plus some others[31] has some physical or mathematical property to recommend them, but each suffers from deficiencies as well. For example, for a given number of pseudonatural orbitals, predicted energies can be poorer when the primitive basis set is expanded.[32]

In the following, we propose a new approach to obtaining an optimized virtual orbital space (OVOS) for energy calculations. Unlike the above methods, we directly employ an energy optimizing principle built upon the second-order Hylleraas functional criteria to obtain a set of $N'_{\rm VIRT} < N_{\rm VIRT}$ orbitals which are linear combinations of all $N_{\rm VIRT}$ orbitals in the basis set. Unlike V^{N-1} orbitals or the usual (not "frozen") pseudonatural orbitals, these OVOS orbitals are chosen to diagonalize the Fock operator for the virtual space, meaning that no modifications to MBPT of CC codes that assume the use of SCF orbitals are required. The CC/MBPT part of our PROPAGATOR program system[33] uses *any* orbital choice,[11,17] but having virtual orbitals that diagonalize the Fock operator is still a computational simplification and might be particularly important for the legion of GAUSSIAN 82[34] users in the community, where SCF orbitals are required in MBPT(= Møller–Plesset) computations. A series of examples using large basis sets and chosen to test the method for $CH_2(^1A_1)$, C_6H_6 and potential surfaces for B_2H_6 and H_2O_2 are reported in the following, after a discussion of the theory.

II. METHODOLOGY

In the initial implementation of the OVOS method we consider a closed shell N electron system. The total Hamiltonian H of the system is partitioned into a zero-order Hamiltonian H_0 being the usual sum of the Hartree–Fock (HF) operators

$$H_0 = \sum_{i=1}^{N} f(i) \tag{1}$$

and the correlation perturbation operator $V = H - H_0$. The sum $E_0 + E_1$ is the HF energy of the system, and E_2, the lowest-order correlation correction. The second-order Hylleraas functional[35] constitutes an upper bound to E_2 for a trial first-order wave function Φ_1,

$$E_2 \leqslant \langle \Phi_1 | H_0 - E_0 | \Phi_1 \rangle + 2\langle \Phi_1 | V - E_1 | \Phi_0 \rangle \equiv J_2. \tag{2}$$

Intermediate normalization of $\Phi^{(0)}$ is assumed, which mandates that the first-order wave function satisfy the following orthogonality condition:

$$\langle \Phi_1 | \Phi_0 \rangle = 0. \tag{3}$$

By varying J_2 with respect to Φ_1 and equating the result

This article is copyrighted as indicated in the article. Reuse of AIP content is subject to the terms at: http://scitation.aip.org/termsconditions. Downloaded to IP: 129.49.170.188 On: Sat, 20 Dec 2014 03:22:48

to zero, one obtains the usual first-order equation from which the first-order wave function can be determined:

$$\frac{\delta}{\delta\Phi_1} J_2 = 2(H_0 - E_0)|\Phi_1\rangle + 2(V - E_1)|\Phi_0\rangle = 0. \quad (4)$$

For the special case of restricting Φ_1 to a sum of excitations of one particle functions[36] and for Φ_0 an SCF wave function, then only two-electron excited determinants contribute to Φ_1:

$$\Phi_1 = \sum_{\substack{i>j \\ a>b}} t_{ij}^{ab}(1)|_{ij}^{ab}\rangle, \quad (5)$$

$$t_{ij}^{ab(1)} = \frac{\langle ab|ij\rangle}{\epsilon_i + \epsilon_j - \epsilon_a - \epsilon_b}.$$

Our usual convention is used where letters $i,j,...$ are used to indicate occupied spin orbitals and $a,b,...$ to indicate virtual spin orbitals, while $p,q,...$ are unrestricted. The set $\{\epsilon_p\}$ are HF orbital energies.

Now, we separate the SCF virtual set into active spin orbitals $(a,b,...)$ and nonactive spin orbitals $(e,f,...)$. The second-order Hylleraas functional is used to find an *optimal rotation* of the active virtual space against the nonactive space, to minimize the second-order correlation energy. We may borrow some of the theory effectively used for MCSCF problems[37,38] to define the orbital rotation by a unitary matrix **U**, represented in an exponential form with an antisymmetric matrix **R**,

$$\phi_a' = \sum_b U_{ba}\phi_b + \sum_e U_{ea}\phi_e, \quad (6)$$

$$\mathbf{U}^\dagger\mathbf{U} = \mathbf{1},$$

$$\mathbf{U}(\mathbf{R}) = \exp(\mathbf{R}),$$

$$\mathbf{R} = -\mathbf{R}^\dagger.$$

A power expansion of the exponential operator is then used,

$$\exp(\mathbf{R}) = \mathbf{1} + \mathbf{R} + \tfrac{1}{2}\mathbf{RR} + \cdots. \quad (7)$$

Since all possible double excitations are present in expansion (5), we can restrict the orbital transformation to only active–nonactive orbital rotations. This happens because the active–active orbital rotations cannot change the second-order energy. Consequently, the following block form is assumed for the **R** matrix:

$$\mathbf{R} = \begin{bmatrix} \mathbf{0} & -\mathbf{R}_{ea} \\ \mathbf{R}_{ae} & \mathbf{0} \end{bmatrix}. \quad (8)$$

An active orbital ϕ_a' after rotation has the following form:

$$\phi_a \to \phi_a' = \phi_a + \sum_e R_{ea}\phi_e - \frac{1}{2}\sum_b\sum_e R_{ea}R_{eb}\phi_b + \cdots. \quad (9)$$

Expressing the second-order functional J_2 for the *reduced* virtual space in terms of active virtual orbitals, we have

$$J_2 = \sum_{i>j} J_{ij}^{(2)}, \quad (10)$$

$$J_{ij}^{(2)} = \sum_{\substack{a>b \\ c>d}} t_{ij}^{ab}(1)t_{ij}^{cd}(1)\,[(f_{ac}\delta_{bd} + f_{bd}\delta_{ac} - f_{ad}\delta_{bc} - f_{bc}\delta_{ad}) - (\epsilon_i + \epsilon_j)(\delta_{ac}\delta_{bd} - \delta_{ad}\delta_{bc})] + 2\sum_{a>b} t_{ij}^{ab}(1)\langle ab|ij\rangle,$$

where the electron-pair separability of the second-order Hylleraas functional has been employed. The matrix element f_{ab} indicates a Fock matrix element. By replacing active orbitals by their rotated form, i.e., using Eq. (9) in Eq. (10), we obtain the Hylleraas functional as a function of rotational parameters. The differentiation of the functional with respect to the rotation parameters leads, then, to first- and second-order derivatives:

$$G_{ea} = \left.\frac{\delta J_2}{\delta R_{ea}}\right|_{\mathbf{R}=\mathbf{0}} \quad \text{(gradient)}, \quad (11a)$$

$$H_{ea,fb} = \left.\frac{\delta^2 J_2}{\delta R_{ea}\delta R_{fb}}\right|_{\mathbf{R}=\mathbf{0}} \quad \text{(Hessian)}. \quad (11b)$$

These can be expressed as follows:

$$G_{ea} = 2\sum_{i>j}\sum_b t_{ij}^{ab}(1)\langle ij|eb\rangle + 2\sum_b D_{ab}^{(2)} f_{eb}, \quad (12a)$$

$$H_{ea,fb} = 2\sum_{i>j} t_{ij}^{ab}(1)\langle ij|ef\rangle - \sum_{i>j}\sum_c [t_{ij}^{ac}(1)\langle ij|bc\rangle + t_{ij}^{cb(1)}\langle ij|ca\rangle]\delta_{ef} + D_{ab}^{(2)}(f_{aa} - f_{bb})\delta_{ef} + D_{ab}^{(2)} f_{ef}(1 - \delta_{ef}), \quad (12b)$$

where $D^{(2)}$ is the second-order density matrix:

$$D_{ab}^{(2)} = \sum_{i>j}\sum_c t_{ij}^{ac}(1)t_{ij}^{bc}(1). \quad (13)$$

Equation (12) has been derived with the assumption that the active orbitals diagonalize the Fock matrix, i.e., are canonical, which may be easily accomplished at each iteration step. It should be noticed that both the gradient and Hessian of J_2 exhibit the same pair separability as the second-order functional itself. It can be seen from Eq. (12) that the **G** and **H** matrices are functions of first-order configuration amplitudes, Fock matrix elements, and two-electron molecular integrals. Only integrals of the kind $\langle$occ(1) occ(2)|virt(1) virt(2)$\rangle$ are involved, which causes the present method to be computationally much simpler and less time consuming than the Rayleigh–Ritz variational principle used in MCSCF orbital optimization techniques. Once the **G** and **H** matrices are determined, the orbital rotation parameters are calculated from the Newton–Raphson equation

$$\mathbf{R} = -\mathbf{G}\cdot\mathbf{H}^{-1}. \quad (14)$$

The application of the Newton–Raphson method to the second-order Hylleraas functional results in the following computational strategy:

(i) Compute the SCF solution.

(ii) Perform a partial transformation of atomic integrals to molecular integrals ($\langle ij|ab\rangle$ type only). The molecular integrals $\langle ij|ab\rangle$ are sorted into a record structure. Each

This article is copyrighted as indicated in the article. Reuse of AIP content is subject to the terms at: http://scitation.aip.org/termsconditions. Downloaded to IP: 129.49.170.188 On: Sat, 20 Dec 2014 03:22:48

TABLE I. MBPT and CC results for the CH_2 ($^1A_1$) molecule calculated with the full and OVOS of various dimensions. A ($9s7p2d\,1f/5s2p$) contracted Gaussian basis set has been used. Energies in a.u. The reference SCF energy is equal to $-38.894\,47$ a.u.

	Correlation energies (percentage of the result in the full space)					
N—number of active virtual orbitals	70 (100%)	46 (65.7%)	35 (50.0%)	22 (31.4%)	12 (17.1%)	8 (11.4%)
MBPT(2)	−0.182 683	−0.180 772 (99.0%)	−0.176 111 (96.4%)	−0.162 049 (88.7%)	−0.116 838 (64.0%)	−0.096 503 (52.8%)
MBPT(3)	−0.204 817	−0.203 261 (99.2%)	−0.199 225 (97.3%)	−0.185 732 (90.7%)	−0.136 710 (66.7%)	−0.114 056 (55.7%)
MBPT(4)	−0.211 884	−0.210 171 (99.2%)	−0.205 881 (97.2%)	−0.192 018 (90.6%)	−0.142 052 (67.0%)	−0.118 725 (56.0%)
CCSDT-1	−0.215 691	−0.213 163 (98.8%)	−0.208 679 (96.7%)	−0.194 551 (90.2%)	−0.144 842 (67.2%)	−0.121 113 (56.2%)
Δ[MBPT(3)] + E_2(exact)		−0.205 173 (100.2%)	−0.205 798 (100.5%)	−0.206 366 (101.2%)	−0.202 555 (98.9%)	−0.200 236 (97.8%)
Δ[MBPT(4)] + E_2(exact)		−0.212 082 (100.1%)	−0.212 453 (100.3%)	−0.212 653 (100.4%)	−0.207 897 (98.1%)	−0.204 905 (96.7%)
Δ[CCSDT-1] + E_2(exact)		−0.215 074 (99.7%)	−0.215 251 (99.8%)	−0.215 186 (99.8%)	−0.210 687 (97.7%)	−0.207 293 (96.1%)

record contains integrals with the same occupied indexes (ij) and all possible virtual indexes (ab).

(iii) Make a selection of an initial active space. The choice is based upon the contribution from each individual virtual orbital to the second-order correlation energy. The contribution is calculated as a sum of the diagonal and a half of the off-diagonal part.

(iv) Transform the molecular integrals $\langle ij|ab\rangle \rightarrow \langle ij|a'b'\rangle$ and compute the first-order amplitudes $t_{ij}^{a'b'}$ (1) for the active virtual orbitals. The integral transformation is not needed in the first iteration.

(v) Construct the gradient and Hessian matrices.

(vi) Solve the Newton–Raphson equation for the orbital rotation parameters **R**. A block generalization of the reduced linear equation technique of Purvis and Bartlett[39] is used. It is recognized that the Hessian matrix is dominated by square blocks located diagonally. A particular block is related to the rotation of all possible active orbitals with one nonactive orbital ($H_{ea,eb}$). Only inverses of all diagonally located blocks are kept in the core.

(vii) Generate the unitary transformation matrix **U** by using the formula[33]

$$\mathbf{U} = \exp(\mathbf{R}) = \mathbf{X}\cosh(\mathbf{d})\mathbf{X}^\dagger + \mathbf{R}\mathbf{X}\sinh(\mathbf{d})\mathbf{d}^{-1}\mathbf{X}^\dagger, \tag{15}$$

where **d** is the square root of a diagonal matrix, which results from the diagonalization of $\mathbf{R}^2$:

$$\mathbf{d}^2 = \mathbf{X}^\dagger\mathbf{R}^2\mathbf{X}. \tag{16}$$

(viii) Construct the Fock matrix for the rotated active space by a simple transformation which involves the orbital energy matrix and the transformation matrix **U**. Next, the Fock matrix is diagonalized to generate new canonical active orbitals.

(ix) Calculate the second-order correlation energy for the new active space. If the energy convergence is satisfactory, the iteration process is terminated, if not a return to (iv) is performed.

As seen, the proposed strategy is, in essence, a two-step optimization procedure. Configuration coefficients are calculated independently from the orbital rotation parameters. Our preliminary experience indicates that the most time consuming step is the solution of the Newton-Raphson linear equation. However, if the block structure of the Hessian is fully exploited, the reduced linear equation method converges quickly.

III. APPLICATIONS AND DISCUSSION

A. CH_2

As a first example of the OVOS method we consider the excited $^1A_1$ state of CH_2. Because this state has some degree of multireference character, higher-order correlation effects measured relative to a single reference function would be expected to be relatively important. Previously, we have reported a series of CC/MBPT results on the singlet–triplet splitting in CH_2 in a variety of basis sets.[40] The largest of these consisted of 74 contracted Gaussian functions defined by Werner and Reinsch,[41] distributed as ($9s7p2d\,1f/5s2p$). The singlet–triplet separation was found to vary by as much as 3.7 mhartree (2.2 kcal/mol) with basis extension at the CCSDT-1 level. The results of our study[40] showed that the SCF energy for the singlet state improved by 7 and 1.5 mhartree, as one changed the basis from ($4s2p1d/2s1p$) to ($6s4p2d/4s2p$) and to ($9s7p2d\,1f/5s2p$), respectively; but the correlation effects as measured at the CCSDT-1 level changed by an important 33.5 and 34.2 mhartree, respectively.

One of the primary reasons for developing the OVOS procedure is to permit the use of much larger basis sets for *correlated* calculations than is currently possible, by reducing the effective dimension of the virtual orbital basis while

This article is copyrighted as indicated in the article. Reuse of AIP content is subject to the terms at: http://scitation.aip.org/termsconditions. Downloaded to IP: 129.49.170.188 On: Sat, 20 Dec 2014 03:22:48

retaining most of the essential correlation effects that would be present in an expanded basis. We can obtain some measure of this by performing a series of OVOS calculations based upon our largest basis but reduced to basis sizes indicative of the different choices of contracted Gaussians made above. These results are shown in Table I.

Of course, the largest percentage of the correlation energy occurs in second order in the correlation perturbation E_2.[5,42] However, by optimizing E_2 for a given number of virtual orbitals, we would expect that a much larger percentage of E_2 could be retained compared to the percentage reduction in the space. This is seen to be the case from Table I, where a reduction in OVOS to 46, i.e., 2/3 of the total, still enables obtaining 99% of E_2. The higher-order corrections tend to be nearly the same as obtained before,[40] resulting in 99.2% of the basis set correlation at the MBPT(4) level, and 98.8% at the CCSDT-1 level. Similarly, a reduction to 50% of the dimension of the entire virtual orbital space, causes a loss of 3.6% in E_2, 2.8% in MBPT(4), and 3.3% in CCSDT-1.

Even a reduction by 1/3 to 22 functions, that is a smaller dimension than a DZP basis, loses only $\sim 11\%$ in E_2 and $\sim 10\%$ at the highest levels. This should be compared with the actual use of a DZP basis for correlated calculations on the CH_2 ($^1A_1$) state. For such a calculation we obtain for the correlation energy $-0.152\,53$ a.u. at the MBPT(4) level and $-0.156\,63$ a.u. for CCSDT-1.[14] Clearly, by taking a much larger initial basis and reducing it to the same size as DZP, we gain about 38 mhartree in the correlation energy or about 64% of the 59 mhartree that would be possible using the full basis. No doubt, much of this is due to the inclusion of f-orbital effects that would not be present in a DZP basis.

The consistency of the higher-order correlation corrections with OVOS, and the fact that the entire E_2 must be computed to define the OVOS anyway (this, however, is only an $\sim n_{\rm occ}^2 N_{\rm virt}^2$ procedure following a restricted, but $\sim n_{\rm occ}^2 N_{\rm VIRT}^3$ transformation to define only the integrals of the form $\langle ij|ab\rangle$) suggests using the exact E_2 with only the higher orders being obtained at the reduced level. These numbers are shown in the bottom three rows of Table I. Hence, in every case from a reduced level of 22 to 46, we obtain almost exactly 100% of the full basis correlation energy as measured by MBPT(3), MBPT(4), or CCSDT-1. This provides an additional improvement, e.g., from using a 22 function OVOS from a 70 function starting point of 59 mhartree (36.7 kcal/mol) in the correlation energy than could be obtained with a slightly larger, though standard DZP basis. It is convenient that unlike MBPT(3) or MBPT(4), CCSDT-1 even shows a bounding property always being slightly less than 100% of the CCSDT-1 correlation energy in the full space, even for this current example where CCSDT-1 is a significant 3 mhartree lower in energy than MBPT(4), and the latter 7 mhartree lower than MBPT(3), both having important effects on the predicted singlet–triplet splitting in CH_2.

With the success of the preceding, we even tried ridiculously low numbers of optimized virtual orbitals, going all the way to less than a DZ level of only 12 and 8 functions. Of course, it is well known that a DZ or smaller basis cannot account for any angular correlation effects because of the absence of polarization functions. However, in the OVOS procedure that is not true, since the polarization functions are mixed into the optimized virtual orbitals weighted as measured by their effect in E_2. For these two cases, corresponding to only 17% and 11% of the excited orbital space, still more than half of E_2 is obtained, and once again, using the exact E_2 enables MBPT(3), MBPT(4), and CCSDT-1 to be within 4% of the full space correlation effects. In some sense, the few correlating functions retained seem to be measuring much of the essential effects of electron correlation.

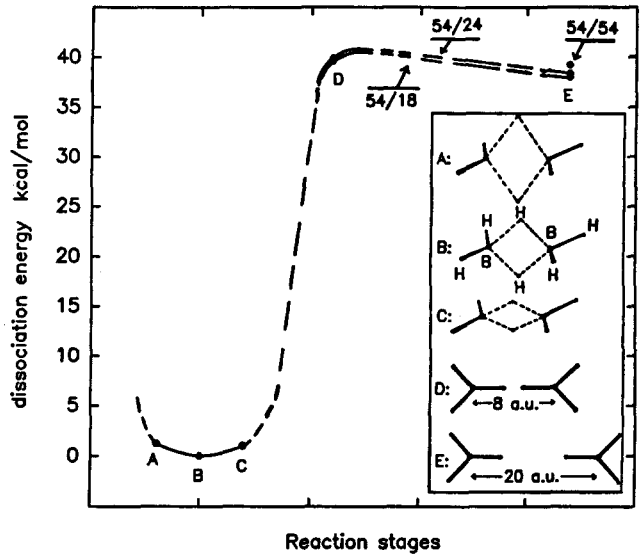

FIG. 1. Dissociation curve for $B_2H_6 \rightarrow 2BH_3$ calculated with [CCSD + T(CCSD)] + E_2(exact) method with different dimensions of OVOS. Reaction stages have been chosen arbitrarily.

B. $B_2H_6 \rightarrow 2BH_3$

In addition to demonstrating that $\sim 100\%$ of the correlation energy can be obtained at a molecule's equilibrium configuration, it is also important to investigate how well the OVOS procedure will work as a function of molecular geometry. Otherwise, predictions of structure and dissociation energies could be in error compared to the full space predictions. To investigate this, we have studied two examples, the dissociation of $B_2H_6 \rightarrow 2BH_3$ and $H_2O_2 \rightarrow 2OH$. In both cases, the diborane "banana" band and the peroxide linkage represent fairly weak chemical bonds $D_0 = 35.5$ and 32.6 kcal/mol, respectively. Also, electron correlation accounts for about half of the dissociation energy.[43]

The main difference in the two examples occur due to the closed-shell diborane molecule dissociating into closed-shell BH_3 units, while H_2O_2 dissociates into open-shell OH radicals. The initial implementation of our OVOS procedure is restricted to the closed-shell RHF reference case, although UHF or two-configuration (TCSCF) extensions are possible. Since for $B_2H_6 \rightarrow 2BH_3$ a closed-shell description is appropriate as a function of any R_{B-B} separation, we should be able to assess the suitability of OVOS as a function of R_{B-B} without any failure of the second-order functional employed to define the OVOS. Since B_2H_6 is actually held together by

This article is copyrighted as indicated in the article. Reuse of AIP content is subject to the terms at: http://scitation.aip.org/termsconditions. Downloaded to IP: 129.49.170.188 On: Sat, 20 Dec 2014 03:22:48

TABLE II. D_e for B_2H_6 at the CCSD + T(CCSD) level, as a function of dimension of the OVOS. Units are kcal/mol. B(1s) electrons are uncorrelated.

Number of active virtual orbitals	CCSD + T(CCSD)	Δ[CCSD + T(CCSD)] + E_2(exact)
54 (complete space)	39.2	39.2
30	36.8	38.8
24	34.6	38.4
18	33.1	38.0

banana bands, however, we define a quasireaction path by defining the five geometries shown in Fig. 1. Using a (4s2p1d/2s1p) contracted Gaussian basis (62 functions), which means the full virtual space contains 54 functions, we consider spaces of size 18, 24, and 30; or 33%, 44%, and 56% of the full dimension. Figure 1 shows the behavior of the energy at the five geometries, chosen to maintain the D_{2h} symmetry of B_2H_6. The barrier, of course, simply arises from choices of geometry and has nothing to do with any barrier in the actual reaction path of $B_2H_6 \rightarrow 2BH_3$.

The CCSD + T(CCSD) model[14] exploits the fact that a final single triple excitation iteration using the T_2 amplitudes (t_{ij}^{ab}) from a converged CCSD calculation is usually a quite accurate approximation to the iterative CCSDT-1 method that allows T_3 amplitudes (t_{ijk}^{abc}) to affect the value of the T_1 and T_2 amplitudes. Since the evaluation of the triple excitation contribution is the rate determining step in most CC/MBPT calculations, T(CCSD) is a much more expeditious model computationally, and for our purposes, will have no significant numerical differences from CCSDT-1[14] or CCSDT.[15]

The slight difference in the dissociation energy (D_e) as a function of the dimension of the OVOS is shown in Table II at the CCSD + T(CCSD) level,[14] and by adding the exact second-order energy. Clearly the latter only introduces an error of 1.2 kcal/mol even for an OVOS of a dimension only one-third as large as the full space. Without the exact E_2 the errors are larger reflecting the fact that most of the important correlation corrections in D_e are recovered at the MBPT(2) level.

Results for the correlation energy of B_2H_6 at equilibrium calculated at various levels and with different numbers of OVOS orbitals are presented in Table III. A comparison with results for $CH_2(^1A_1)$ shows somewhat poorer convergence. At about 50% reduction, even a partly multireference problem like $CH_2(^1A_1)$ shows ~5% better agreement, yet once again, almost all of the difference shows up in second order. Hence, once the exact E_2 is added to the higher-order OVOS corrections, nearly perfect agreement with the best correlation correction is achieved. Although B_2H_6 does not show particularly poor convergence as judged by the differences in the infinite-order CCSD vs its fourth-order SDQ-MBPT(4) approximation ($\Delta E = 0.5$ mhartree), e.g., which is contrary to $CH_2(^1A_1)$ [$\Delta E = 2$ mhartree for CCSD-SDQ(4)] and [$\Delta E = 4$ mhartree for CCSDT-1-STDQ(4)], it is probable that the larger initial basis for the latter molecule leads to better OVOS results for the correlation energy. The interplay between size of the initial basis and the accuracy of the OVOS correlation predictions should be studied in future work.

Some actual FPS timings for B_2H_6 calculations are shown in Table IV, showing that even for a modest DZP basis calculation a factor of 4.4 to 9.3 may be gained at the CCSD level by using OVOS of 30 to 18 functions. The net gain factor includes the fact that less iterations are required to converge to the same threshold once the number of orbitals is reduced from the full space of 54. For example, 20 iterations are required in the full space, while only 12 are needed for an OVOS of dimension 30, and 11 in the other cases. Only a single triple excitation evaluation is used in T(CCSD) as discussed above, so even though it requires more time than a CCSD iteration, as it is only evaluated once, only modest additional savings over the CCSD time are possible for this example.

TABLE III. MBPT and CC calculations for B_2H_6 at its experimental equilibrium geometry ($R_{B-B} = 1.77$ Å, $R_{B-H_b} = 1.33$ Å, $R_{B-H_t} = 1.19$ Å, $\angle H_tBH_t = 120°$).[a]

N—number of active V_0	54 full space	30 (55.6%)	24 (44.4%)	18 (33.3%)
MBPT(2)	−0.218 413	−0.199 649 (91.4%)	−0.184 548 (84.5%)	−0.158 765 (72.7%)
MBPT(3)	−0.254 338	−0.235 298 (92.7%)	−0.218 236 (85.8%)	−0.187 968 (73.9%)
CCSD	−0.260 142	−0.242 208 (93.1%)	−0.224 941 (86.5%)	−0.194 967 (74.9%)
CCSD + T(CCSD)	−0.266 361	−0.246 581 (92.6%)	−0.228 759 (85.9%)	−0.197 956 (74.3%)
Δ[MBPT(3)] + E_2(exact)		−0.254 462 (100.0%)	−0.252 101 (99.1%)	−0.247 616 (97.4%)
Δ[CCSD] + E_2(exact)		−0.260 972 (100.3%)	−0.258 806 (99.5%)	−0.254 615 (97.9%)
Δ[CCSD + T(CCSD)] + E_2(exact)		−0.265 345 (99.6%)	−0.262 624 (98.6%)	−0.257 604 (96.7%)

[a] Electrons in B(1s) orbitals are uncorrelated.

This article is copyrighted as indicated in the article. Reuse of AIP content is subject to the terms at: http://scitation.aip.org/termsconditions. Downloaded to IP: 129.49.170.188 On: Sat, 20 Dec 2014 03:22:48

TABLE IV. B_2H_6 ($4s2p1d/2s1p$) D_{2h}. FPS 164 max timings (s) for OVOS calculations, $R_{B\text{-}B} = R_{eq}$.

N	54 = full space	30	24	18
CCSD(per iteration)	512	175(34%)	127(25%)	89(17%)
T(CCSD)	696	120(17%)	67(9.6%)	32(4.6%)
OVOS generation		212	202	98
CCSD (net gain-all its.)		×4.4	×6.4	×9.5
CCSD + T(CCSD) (net gain)		×4.5	×6.6	×9.9

C. $H_2O_2 \rightarrow 2OH$

For H_2O_2 in a ($4s3p1d/2s1p$) contracted Gaussian basis, the peroxide bond is broken while keeping the R_{OH} distance and OOH angle fixed ($R_{OH} = 1.795$ bohr; $\measuredangle OOH = 94.8°$[17,18]), while the two OH bonds are kept at the *gauche* configuration (i.e., C_2) that is experimentally observed with a dihedral angle = 111.5°.

The CCSDT-1 potential curves at various sizes of optimized orbital space 7, 14, and 21 which, respectively, account for 18%, 36%, and 54% of the total of 39 orbitals are illustrated in Fig. 2. All calculations employ a restricted Hartree–Fock (RHF) reference, hence, the reference function does not correctly separate into two open-shell $^2\Sigma$ OH radicals, but instead goes to a much higher asymptote that is an average of OH^+ and OH^-. This places a severe constraint on any single RHF reference approach for electron correlation yet the CCSDT-1 model, as shown in Fig. 2, still correctly separates H_2O_2 into two OH radicals. Any lower level of perturbation theory approximation such as MBPT(4) is not able to handle this type of dissociation, however, since one virtual and one occupied orbital are becoming degenerate as the bond is broken. This causes the RHF perturbation theory denominators to become singular at infinite separation, and to show a near singularity in the bond breaking region, which causes MBPT(4) or any lower level of MBPT to approach minus infinity at infinite separation. Even though MBPT(4) is the fourth-order approximation to CCSDT-1, the remaining infinite-order terms introduced in CCSDT-1 enable the method to overcome the approaching denominator singularity. One way to understand this is that unlike perturbation theory, CC theory is invariant to the splitting of the Hamiltonian into H_0 and V, and one can conceive of other choices of H_0 that would avoid the singularities. CCSD will also provide a reasonable curve all the way to dissociation, but will be too high, reflecting its more limited ability to overcome the erroneous behavior of the RHF reference.[11] Hence triples are essential in CC to obtain a good potential curve for the breaking of a single bond, at least subject to the usual SCF orbitals.

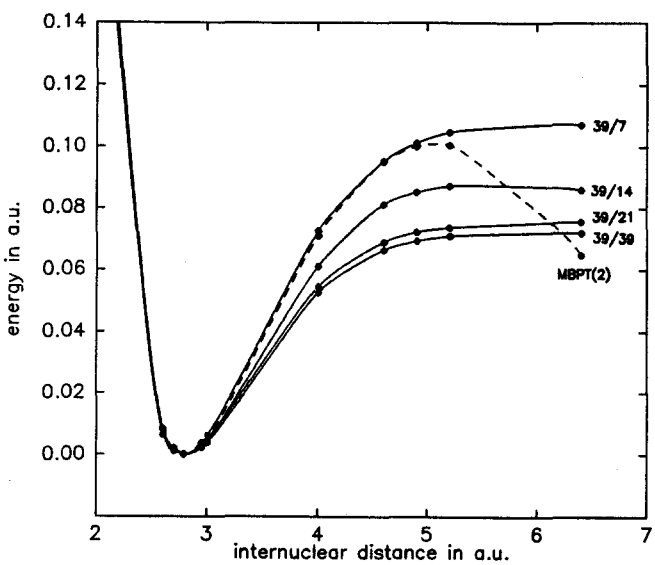

FIG. 2. Dissociation of the H_2O_2 molecule calculated with the CCSDT-1 method. The horizontal axis indicates the HO--OH separation, with the dihedral angle kept at a constant 111.5°. N_{VIRT}/N_{VIRT} symbols indicate the virtual space reduction levels. The minima for all curves has been fixed at the same level on the energy axis. For comparison, the dissociation curve obtained at the MBPT(2) level with the complete virtual space is shown, to indicate where the Hylleraas functional breaks down for this example.

As mentioned above, the current implementation of the OVOS scheme is limited to RHF cases and is based upon MBPT(2); so it, too, should suffer as MBPT(2) misbehaves in the bond breaking region. This is reflected in the potential curves for H_2O_2. Although very similar in the vicinity of equilibrium—R_{oo} is predicted to be 2.82 for the full 39 orbital space, 2.81 for $N = 21$, 2.80, for $N = 14$, and 2.78 for $N = 7$—progressively poorer bond dissociation energies are obtained as a function of the size of the OVOS, ranging from an error of 2 kcal/mol for $N = 21$ to 9 for $N = 14$ and 22 for $N = 7$. In Fig. 2, a dashed line superimposes the full space MBPT(2) upon the potential curves, showing how the eroneous behavior of the second-order functional parallels the OVOS curves. Considering the atrocious behavior of MBPT(2) beyond ~5 bohr, it is surprising that the optimized virtual orbitals obtained from the second-order functional are as good as they are. Of course, the OVOS procedure can be readily generalized to a two-configuration RHF case, then there should be no problem with using it for singly bonded molecules that separate into open-shell fragments. A generalization to an unrestricted Hartree–Fock (UHF) OVOS method could also be made, to be consistent with the large number of calculations that employ UHF references to make a single determinant reference correctly separate into open-shell fragments. Ultimately, of course, even a more general MCSCF procedure could constitute a reference for OVOS to study multiple bond breaking, for example.

Energy results are shown at the intermediate R_{oo} distance of 4.6 bohr in Table V. Despite the comparative poorness of the MBPT(2) energy, the behavior there is very similar to that previously observed for CH_2 and B_2H_6. Of course,

This article is copyrighted as indicated in the article. Reuse of AIP content is subject to the terms at: http://scitation.aip.org/termsconditions. Downloaded to IP: 129.49.170.188 On: Sat, 20 Dec 2014 03:22:48

TABLE V. MBPT and CC calculations for H_2O_2 at $R_{oo} = 4.6$ bohr.[a]

N—number of active V_0	39 full space	21	14	7
MBPT(2)	−0.497 204	−0.463 585 (93.2%)	−0.393 750 (79.2%)	−0.303 846 (61.1%)
MBPT(3)	−0.494 100	−0.460 921 (93.3%)	−0.385 915 (78.1%)	−0.293 581 (59.4%)
MBPT(4)	−0.553 396	−0.512 983 (92.7%)	−0.428 949 (77.5%)	−0.316 327 (57.2%)
CCSDT-1	−0.548 625	−0.508 981 (92.8%)	−0.427 915 (78.0%)	−0.316 259 (57.6%)
Δ[MBPT(3)D] + E_2(exact)		−0.494 540 (100.9%)	−0.489 369 (99.0%)	−0.486 939 (98.6%)
ΔMBPT(4) + E_2(exact)		−0.546 602 (98.8%)	−0.532 403 (96.2%)	−0.509 685 (92.1%)
Δ[CCSDT-1] + E_2(exact)		−0.542 600 (98.9%)	−0.531 369 (96.9%)	−0.509 617 (92.9%)

[a] Electrons in O(1s) orbitals are uncorrelated.

beyond ~5 bohr MBPT(2) becomes much to low in the bond breaking region, so it would be inappropriate to add the exact E_2 to the OVOS higher-order correlation energy results in that region.

In terms of computer timings shown in Table VI, a few points should be noted. Even for a smaller basis the lower symmetry in H_2O_2 (which is only used passively by our CC/MBPT codes) plus larger numbers of electrons causes the CCSD iterations to be slower. Second, unlike the B_2H_6 example, here we report CCSDT-1 results and it is apparent that the iterative inclusion of triple excitations via CCSDT-1 adds greatly to the time required for the calculation. Unlike a single iteration of triples as in T(CCSD), we have two $\sim n_{\rm occ}^3 N_{\rm VIRT}^4$ steps per iteration in CCSDT-1 and somewhat poorer coding for the latter, which causes a CCSDT-1 iteration to be almost a factor of 10 larger than for CCSD. This does enable the savings from OVOS to be far more dramatic, with close to two orders of magnitude (83) gained in the time for the smallest basis. Once again, in the process of reducing the space, we seem to obtain a set of orbitals that provide a better essential description of electron correlation. Consequently, for the iterative CC methods, we require fewer iterations for the optimized virtual space to converge the energy to the same threshold than for the full space. (The full space CCSDT-1 calculation requires 19 iterations, while CCSDT-1 calculations with the virtual space reduced to 21, 14, and 7 orbitals require 14, 12, and 11 iterations, respectively.) Considering the time required for each CCSDT-1 iteration, our savings in net time for the calculation can be far greater than the already very significant factors associated with the virtual orbital reduction. The greater time required to generate the OVOS orbitals for $N'_{\rm VIRT} = 14$ compared to $N'_{\rm VIRT} = 21$, simply reflects the greater number of iterations incurred by OVOS from starting from a poorer initial guess.

D. C_6H_6

As an illustration that is more typical of those planned in the future, which simply could not be attempted without OVOS, we have considered benzene in a DZP basis set of 126 contracted Gaussian orbitals ($N_{\rm VIRT} = 105$). If all the symmetry in C_6H_6 were completely exploited, CC calculations would require a modest amount of computer time. The current CC/MBPT part of our PROPAGATOR code[33] uses symmetry passively, by not processing integrals or evaluating cluster amplitudes that are zero by symmetry, but does not evaluate only the symmetry unique amplitudes, so our current observations will be fairly indicative of most 36 electron ~100 basis calculations. [The C(1s) electrons are uncorrelated.] For CCSD, an $\sim n_{\rm occ}^2 N_{\rm VIRT}^4 \times N_{\rm ITS}$ procedure, this is still a reasonable, but large scale correlated calculation for our FPS 164. However, with our current code, even a single iteration of triple excitations to evaluate T(CCSD) is a quite demanding step, and CCSDT-1 would be prohibitive.

However, once we obtain an OVOS of dimension 30; or some 29% of the entire space, we are able to easily carry out CCSDT-1 calculations. The numbers are shown in Table VII, which we estimate took less than a hundreth of the time which the full CCSDT-1 result would require. The result of −231.594 456 a.u. of the valence correlation energy of −0.862 00 a.u. for the DZP basis would be expected to be

TABLE VI. H_2O_2 (4s2p1d/2s1p) C_2. FPS 164 timings (s) for OVOS calculations, $R_{oo} = 4.6$ bohr.

N	39 = full space	21	14	7
CCSD (per iteration)	626	151(23%)	64(10%)	52(6%)
CCSDT-1 (per iteration)	5909	797(13.5%)	288(4.9%)	110(1.9%)
Orbital generation		323	409	127
CCSD (net gain-all its.)		×5	×10	×17
CCSDT-1 (net gain-all its.)		×9	×29	×83

This article is copyrighted as indicated in the article. Reuse of AIP content is subject to the terms at: http://scitation.aip.org/termsconditions. Downloaded to IP: 129.49.170.188 On: Sat, 20 Dec 2014 03:22:48

TABLE VII. C_6H_6 (126 fxns. 105 virtual). Comparison of MBPT and CC results for the correlation energy for the full basis and an OVOS of dimension 30. Experimental geometry. DZP basis SCF = −230.732 556.[a]

	OVOS(30)	Δ[OVOS(30)] + E_2(exact)	Full space (105)
MBPT(2)	−0.534 605 (68%)	−0.785 964 (100%)	−0.785 964
E_3	−0.024 699		−0.033 877
MBPT(3)	−0.559 304	−0.810 663 (99%)	−0.819 841
$E_4(D)$	−0.014 612		−0.020 251
$E_4(S)$	−0.002 787		−0.005 200
$E_4(T)$	−0.016 174 (42%)		−0.038 180
$E_4(Q)$	+0.010 698 (48%)		+0.022 3105
MBPT(4)	−0.582 179 (71%)	−0.833 538 (101%)	−0.822 916
CCSD	−0.568 954 (69%)	−0.821 021 (99%)	−0.825 563
CCSD + T(CCSD)	−0.584 656 (68%)	−0.836 840 (97%)	−0.861 900
CCSDT-1	−0.584 640	−0.836 000	...

[a] Electrons in C(1s) orbitals are left uncorrelated.

~60% of the exact valence correlation energy.

The triple excitation effect in C_6H_6 as measured by their fourth-order contribution is −38.2 mhartree, while the contribution from CI quadruple excitation contributions is approximately $E_4(Q) + E_2\langle\phi_1|\phi_1\rangle = -212$ mhartree,[44] where ϕ_1 is the first-order MBPT wave function. The second term corresponds to the fourth-order unlinked diagrams that would remain in a CI until *all* quadruple excitations are included, while the first is the contribution from the linked quadruple excitation diagrams. Hence, CI quadruple excitations would account for ~25% of the correlation energy with an additional ~4.4% for triple excitations. Such a large percentage of the correlation energy coming from higher than double excitations attests to the well-known advantages of many-body methods for handling the correlation problem for larger molecules.[5,42]

For C_6H_6, one negative aspect of the OVOS procedure is the poorer estimate of the triple and linked quadruple excitations. Although an OVOS of 30 obtains 71% of MBPT(4), and 101% once the exact E_2 is included, for the quadruple and time consuming triple excitations only 48% and 42% of the exact value is recovered. Though often an essential part of the correlation in predictive quantum chemistry, and ~4% of the correlation energy for this example, due to triple and quadruple excitation diagrams, numerically this is still a small enough part of the whole correlation energy that 101% is recovered for the MBPT(4) energy, with an overestimate of 10 mhartree. The CCSD method does better, with Δ[CCSD] + E_2(exact) being 5.5 mhartree away from the full basis result. T(CCSD), with an OVOS of 30, is still about 20 mhartree from the full basis result. It would appear that although an OVOS generated from second-order perturbation theory does a good job with correlation overall, the orbitals are not ideal for other, essentially different correlation effects such as those due to triple excitations. Other methods based upon an infinite-order Bethe–Goldstone cluster decomposition have shown a better behavior in numerical basis CC calculations.[45]

IV. CONCLUSION

This paper has presented a method (OVOS) for obtaining a second-order correlation energy optimum set of $N'_{\rm VIRT} < N_{\rm VIRT}$ orbitals for high-level correlated calculations. As long as the second-order energy is the largest part of the correlation energy and is properly behaved, this set of orbitals should be nearly the best possible set of the chosen dimension for the *energy* of the lowest state of that symmetry. The orbitals are chosen to diagonalize the Fock operator, so they may be used with the same simplicity as the canonical virtual orbitals in correlated calculations. On the other hand, some argument can be made for not diagonalizing the Fock operator if different numbers of orbitals are used for different levels of excitation.[30] Elsewhere, we will report detailed comparisons with pseudonatural orbitals[25] and other potential alternative choices.[18,26]

When the dimension of the OVOS is a small fraction of that for the full virtual space, there is an inevitable loss in the second-order correlation energy, though much less than the percent reduction in the space, yet the total energy effect of higher correlation corrections tends to be relatively constant. Hence, adding the exact E_2, which is a byproduct of the OVOS generation procedure, enables recovering nearly 100% of the correlation energy even for examples where the OVOS dimension is quite small. Futhermore, by reducing the dimension of the virtual orbital space, we obtain better convergence for CC methods resulting in additional important savings in computations beyond the already dramatic savings achieved by the smaller dimension of the correlating orbital space. Apparently, a few very well chosen correlating orbitals suffice for most of the higher-order correlation effects on the energy.

For properties like excitation energies[46] or other properties than the energy,[47] there is less reason to believe that the OVOS energy optimum orbitals would be a particularly appropriate choice. However, the same computational procedure could be used to employ the Hylleraas principle for

This article is copyrighted as indicated in the article. Reuse of AIP content is subject to the terms at: http://scitation.aip.org/termsconditions. Downloaded to IP: 129.49.170.188 On: Sat, 20 Dec 2014 03:22:48

some other property, perhaps the polarizability, e.g., to provide orbitals that might be more appropriate for high-level correlated studies of moments, polarizabilities, and hyperpolarizabilities.[47] For such a case, it would appear to be appropriate to use either a finite-field procedure that adds the perturbation to the Hamiltonian[47] or to use two coupled simultaneous optimizations,[48] one for the correlation energy and the other for the property to generate orbitals to best describe the net correlation effects for some such property. In particular, the orbital contributions allowed by symmetry for the polarizability and the correlation energy will be quite different and must be properly introduced into the computation.

The best way to use the OVOS procedure would be for correlated calculations which could not be done in the conventional way because of the excessive dimension of the N_{VIRT} space. In particular, SCF calculations are being done routinely that use >300 basis functions,[49] yet $N_{\mathrm{VIRT}} \simeq 100$ would be about the effective limit for most high-level correlated calculations today, even on supercomputers. A tool like OVOS can potentially make it possible to exploit the full dimension of the SCF basis augmented by even greater numbers of polarization functions in high-level correlated calculations with potentially modest losses in accuracy, compared to the full basis results. Consequently, numerically important effects such as those due to triple excitation contributions could be included even for very large basis calculations. In fact, the OVOS method could conceivably be used to extrapolate a correlated contribution to the basis set limit.

The recent wealth of experimental results emerging for anions,[50,51] which are known to be among the most difficult systems to describe in *ab initio* applications because of the limited number of conventional GTO basis functions which can be employed for these highly diffuse systems, represent a natural class of applications of the OVOS technique. Correlation is essential for predictive results on such anions, but except for a few studies we have made for diatomic systems that alone permit the use of a numerical orbital basis set to attempt to transcend the basis set limitation,[52] there has been no suitable approach to employing enough functions in correlated calculations on polyatomic anions to be confident of the results obtained. Perhaps the OVOS procedure will facilitate such studies.

As we have shown, the OVOS method even restricted to an RHF reference is quite good as a function of geometry, but the one procedure that could be potentially better than OVOS for any point on a potential energy surface might be a multireference or MCSCF generalization of the procedure. This would have the advantage of including the "nondynamic" correlation effects at most choices of internuclear separation. However, even a multireference generalization would still benefit from being based upon the Hylleraas second-order functional for introducing the "dynamic" correlation effects since this procedure offers a much simpler coupling among orbitals than a Rayleigh–Ritz variational procedure.

The OVOS method lends itself well to a routinely generated "black-box" procedure for obtaining orbitals for MBPT, CC, or CI calculations, and we are in the process of using the method to treat states of large molecules, some of biochemical interest, at levels of sophistication not previously attempted.

ACKNOWLEDGMENTS

We appreciate the assistance of Dr. Sam Cole in performing some of the reference calculations reported here. This work has been supported by the U.S. Office of Naval Research.

[1] R. Pauncz, in *Alternant Molecular Orbital Theory* (Saunders, Philadelphia, 1967), pp. 7–8
[2] (a) P. Saxe, H. F. Schaefer III, and N. C. Handy, Chem. Phys. Lett. **79**, 202 (1981); (b) R. J. Harrison and N. C. Handy, *ibid.* **95**, 386 (1983).
[3] (a) C. W. Bauschlicher, Jr., S. R. Langhoff, P. R. Taylor, and H. Partridge, Chem. Phys. Lett. **126**, 436 (1986); (b) C. W. Bauschlicher, Jr. and P. R. Taylor, J. Chem. Phys. **85**, 2779 (1986); (c) C. W. Bauschlicher, Jr., S. R. Langhoff, P. R. Taylor, N. C. Handy, and P. J. Knowles, *ibid.* **85**, 1469 (1986).
[4] R. L. Graham, D. C. Yeager, J. Olsen, P. Jørgensen, R. Harrison, S. Zarrabian, and R. J. Bartlett, J. Chem. Phys. **85**, 6544 (1986).
[5] R. J. Bartlett, Annu. Rev. Chem. **32**, 359 (1981), and references therein.
[6] R. J. Bartlett and D. M. Silver, Int. J. Quantum Chem. Symp. **8**, 271 (1974); Chem. Phys. Lett. **29**, 199 (1974).
[7] R. J. Bartlett, H. Sekino, and G. D. Purvis III, Chem. Phys. Lett. **98**, 66 (1983).
[8] M. J. Frisch, R. Krishnan, and J. A. Pople, Chem. Phys. Lett. **75**, 66 (1980).
[9] J. Cizek, J. Chem. Phys. **45**, 4256 (1969); Adv. Chem. Phys. **14**, 35 (1969).
[10] R. J. Bartlett and G. D. Purvis III, Int. J. Quantum Chem. **14**, 561 (1978); Phys. Scr. **21**, 255 (1980).
[11] S. J. Cole and R. J. Bartlett, J. Chem. Phys. **86**, 873 (1986).
[12] G. D. Purvis III and R. J. Bartlett, J. Chem. Phys. **76**, 1910 (1982).
[13] Y. S. Lee, S. A. Kucharski, and R. J. Bartlett, J. Chem. Phys. **81**, 5906 (1984); **82**, 5761 (E) (1985).
[14] M. Urban, J. Noga, S. J. Cole, and R. J. Bartlett, J. Chem. Phys. **83**, 4041 (1985).
[15] J. Noga and R. J. Bartlett, J. Chem. Phys. **86**, 7041 (1987).
[16] (a) R. Shepard, I. Shavitt, and J. Simons, J. Chem. Phys. **76**, 543 (1982); (b) H. Lischka, R. Shepard, F. B. Brown, and I. Shavitt, Int. J. Quantum Chem. Symp. **15**, 91 (1981); (c) P. E. M. Siegbahn, J. Almlöf, A. Heiberg, and B. O. Roos, J. Chem. Phys. **74**, 2384 (1981).
[17] W. D. Laidig, G. D. Purvis III, and R. J. Bartlett, J. Phys. Chem. **89**, 2161 (1985); Int. J. Quantum Chem. Symp. **16**, 561 (1982).
[18] (a) D. M. Silver and R. J. Bartlett, Phys. Rev. A **13**, 1 (1976); (b) D. M. Silver, S. Wilson, and R. J. Bartlett, Phys. Rev. **16**, 477 (1977).
[19] (a) T. L. Gilbert, J. Chem. Phys. **43**, 5248 (1985); (b) G. Das and A. C. Wahl, *ibid.* **44**, 87 (1966).
[20] (a) P. O. Löwdin, Phys. Rev. **97**, 1474 (1955); (b) E. R. Davidson, J. Chem. Phys. **57**, 2005 (1972); E. R. Davidson and C. F. Bender *ibid.* **56**, 4334 (1972).
[21] R. C. Haddon, C. E. Brus, and K. Raghavachari, Chem. Phys. Lett. **125**, 459 (1986).
[22] H. P. Kelly, *Perturbation Theory and its Application in Quantum Mechanics*, edited by C. H. Wilcox (Wiley, New York, 1966), pp. 215–241.
[23] H. J. Silverstone and M. L. Yin, J. Chem. Phys. **49**, 2020 (1968).
[24] S. Huzinaga and C. Arnau, Phys. Rev. A **1**, 1258 (1970).
[25] (a) W. Meyer, J. Chem. Phys. **58**, 1017 (1973); (b) P. J. Hay *ibid.* **59**, 2468 (1973).
[26] T. L. Barr and E. R. Davidson, Phys. Rev. A **1**, 64 (1970).
[27] E. R. Davidson, J. Chem. Phys. **57**, 1999 (1972).
[28] W. J. Hunt and W. A. Goddard III, Chem. Phys. Lett. **3**, 414 (1969).
[29] (a) I. L. Cooper and C. N. M. Pounder, J. Chem. Phys. **77**, 5045 (1982); (b) S. Bird and T. A. Claxton, *ibid.* **80**, 3742 (1984); (c) W. L. Luken and B. A. B. Seiders, Chem. Phys. **92**, 235 (1985); (d) F. Illas, M. Merchan, M. Pelissier, and J. P. Malrieu, Chem. Phys. **107**, 361 (1986).
[30] D. Feller and E. R. Davidson, J. Chem. Phys. **74**, 3977 (1981).
[31] P. Fantucci, V. Bonačić-Koutechký, and J. Koutecký, J. Comput. Chem. **6**, 462 (1985).

This article is copyrighted as indicated in the article. Reuse of AIP content is subject to the terms at: http://scitation.aip.org/termsconditions. Downloaded to IP: 129.49.170.188 On: Sat, 20 Dec 2014 03:22:48

[32]G. Karlström, B. Jönsson, B. O. Roos, and P. E. M. Siegbahn, Theor. Chim. Acta. **48**, 59 (1978).
[33]PROPAGATOR program system consists of the molecule integral program of J. Almlöf, GRNFNC that does SCF calculations and integral transformation of G. Purvis; and CC/MBPT for coupled-cluster and many-body perturbation theory calculations, written by R. J. Bartlett, G. D. Purvis, Y. Lee, S. J. Cole, and R. Harrison.
[34]J. S. Binkley, M. J. Frisch, D. J. DeFrees, K. Raghavachari, R. A. Whiteside, H. B. Schlegel, E. M. Fluder, and J. A. Pople, GAUSSIAN 82, Carnegie-Mellon University, Pittsburgh, 1983.
[35]E. A. Hylleraas, Z. Phys. **54**, 347 (1929).
[36]L. Adamowicz and R. J. Bartlett, Int. J. Quantum Chem. **26**, 213 (1984).
[37](a) E. Dalgaard and P. Jørgensen, J. Chem. Phys. **69**, 3833 (1978); (b) E. Dalgaard, Chem. Phys. Lett. **65**, 559 (1979).
[38](a) R. Shepard and J. Simons, Int. J. Quantum Chem. Symp. **14**, 211 (1980); (b) B. H. Lengsfield, J. Chem. Phys. **73**, 382 (1980); (c) H.-J. Werner, *ibid.* **73**, 3342 (1980).
[39]G. D. Purvis III and R. J. Bartlett, J. Chem. Phys. **75**, 1284 (1981).
[40]S. J. Cole and R. J. Bartlett, Chem. Phys. Lett. **113**, 271 (1985).
[41]H.-J. Werner and E.-A. Reinsch, J. Chem. Phys. **76**, 3144 (1982).
[42]R. J. Bartlett and G. D. Purvis III, Ann. N. Y. Acad. Sci. **367**, 62 (1981).
[43]L. T. Redmon, G. D. Purvis III, and R. J. Bartlett, J. Am. Chem. Soc. **101**, 2856 (1979).
[44]R. J. Bartlett, I. Shavitt, and G. D. Purvis III, J. Chem. Phys. **71**, 281 (1979).
[45](a) L. Adamowicz, R. J. Bartlett, and E. A. McCullough, Phys. Rev. Lett. **54**, 426 (1985); (b) L. Adamowicz and R. J. Bartlett, J. Chem. Phys. **84**, 6837 (1986).
[46]J. Oddershede and J. R. Sabin, J. Chem. Phys. **79**, 2295 (1983).
[47](a) R. J. Bartlett and G. D. Purvis III, Phys. Rev. A **20**, 3 (1979); (b) H. Sekino and R. J. Bartlett, J. Chem. Phys. **84**, 2726 (1986).
[48]A. Mukherjee and M. Karplus, J. Chem. Phys. **38**, 44 (1963).
[49](a) J. Almlöf, K. Faegri, Jr., and K. Kusell, J. Comp. Chem. **3**, 385 (1982); (b) H. P. Lĵhi, J. H. Ammeter, J. Almlöf, and K. Faegri, Jr., J. Chem. Phys. **77**, 2002 (1982).
[50]R. N. Compton, P. W. Reinhardt, and C. D. Cooper, J. Chem. Phys. **68**, 4360 (1978).
[51]D. G. Leopold, K. K. Murray, and W. K. Lineberger, J. Chem. Phys. **81**, 1048 (1984).
[52]L. Adamowicz and R. J. Bartlett, J. Chem. Phys. **83**, 6268 (1985).

This article is copyrighted as indicated in the article. Reuse of AIP content is subject to the terms at: http://scitation.aip.org/termsconditions. Downloaded to IP: 129.49.170.188 On: Sat, 20 Dec 2014 03:22:48